



# Manufacturing of the bulk amorphous $\text{Fe}_{61}\text{Co}_{10}\text{Zr}_{2+x}\text{Hf}_{3-x}\text{W}_2\text{Y}_2\text{B}_{20}$ alloys (where $x = 1, 2, 3$ ) their microstructure, magnetic and mechanical properties

Marcin Nabialek<sup>a</sup>, Marcin Dospial<sup>a,\*</sup>, Michal Szota<sup>b</sup>, Jacek Olszewski<sup>a</sup>, Simon Walters<sup>c</sup>

<sup>a</sup> Institute of Physics, Czestochowa University of Technology, 19 Armii Krajowej Av., 42 200 Czestochowa, Poland

<sup>b</sup> Institute of Material Science Engineering, Czestochowa University of Technology, 19 Armii Krajowej Av., 42 200 Czestochowa, Poland

<sup>c</sup> University of Brighton, Engineering Research Centre, Lewes Road, Brighton, United Kingdom

## ARTICLE INFO

### Article history:

Received 28 July 2010

Received in revised form 20 January 2011

Accepted 20 January 2011

Available online 2 March 2011

### Keywords:

Amorphous material

Metallic glasses

Nanostructured material

Rapid-solidification

Magnetization

Mechanical properties

Microstructure

Magnetic measurements

Mössbauer spectroscopy

Scanning electron microscopy

X-ray diffraction

## ABSTRACT

In this paper the microstructure, magnetic properties and mechanical studies results for  $\text{Fe}_{61}\text{Co}_{10}\text{Zr}_{2+x}\text{Hf}_{3-x}\text{W}_2\text{Y}_2\text{B}_{20}$  (for  $x = 1, 2$  or  $3$ ) alloys are presented. The samples used in the investigations were obtained by a suction-casting method. The samples were produced in the forms of rods with diameter of 1 mm and length of about 20 mm and plates with thickness of 0.5 mm and surface area of about 100 mm<sup>2</sup>. The results show that the best soft magnetic properties were achieved by  $\text{Fe}_{61}\text{Co}_{10}\text{Zr}_3\text{Hf}_2\text{W}_2\text{Y}_2\text{B}_{20}$  amorphous alloy in the form of a plate. This sample has the highest value of saturation magnetization (1.09 T) and the smallest values of coercivity ( $H_C = 1.5$  A/m) and core losses. All investigated samples of amorphous alloys were characterized by substantially greater values of microhardness and, unfortunately, slightly lower values of wear resistance compared with their crystalline counterparts.

© 2011 Elsevier B.V. All rights reserved.

## 1. Introduction

During the last 20 years there have been extensive investigations of bulk amorphous alloys [1–3]. The earliest paper related to the subject of 3-d transition metal base amorphous alloys appeared in 1997 and featured the group of Fe–Co–(Zr, Nb, Ta)–(Mo, W)–B alloys [4,5]. Materials, in which the base elements are Fe–Co–B, exhibit good glass forming ability (GFA), very good thermal stability of the amorphous phase, much better mechanical properties (hardness and wear resistance) and higher corrosion resistance in comparison with their classical, crystalline counterparts [6–8].

This group of materials exhibits excellent performance parameters for a relatively low production cost, given the achieved technical parameters. This makes them highly suitable in specialist applications, e.g. military industries, sports industries, and medical instruments, to name but a few. In addition, these materials exhibit excellent soft magnetic properties (i.e. large values of saturation magnetization and permeability, low values of coercivity and

core losses) [9,10]. In fact, these alloys have already found an application as a material for transformer cores in the electrotechnical industry [11]. The predominant method for producing amorphous materials, so-called melt-spinning, requires high cooling velocities of about 10<sup>6</sup> K/s and only facilitates production of thin ribbons with thicknesses of less than 100 μm. Bulk amorphous alloys can be obtained using a much lower cooling velocity, i.e. less than 10<sup>3</sup> K/s, by means of: suction-casting and injection-casting methods. These methods facilitate the production of alloys in different shapes and thicknesses of greater than 100 μm.

This paper presents the results of studies of  $\text{Fe}_{61}\text{Co}_{10}\text{Zr}_{2+x}\text{Hf}_{3-x}\text{W}_2\text{Y}_2\text{B}_{20}$  (where  $x = 1, 2$  or  $3$ ) bulk amorphous alloys. All samples of the investigated alloys were examined in the as-cast state.

## 2. Experimental

Ingots of the investigated alloys were produced from the high purity elements: Fe, 99.98; Y, 99.99; Nb, 99.999. Boron was added to the alloy as a FeB ingot with known composition. Samples were obtained using a suction-casting method, which allowed the production of bulk amorphous alloys. The ingots were produced by the arc-melting of all components and re-melted several times in order to obtain an homogenous material. Pure titanium was used as a getter in a production process.

\* Corresponding author. Tel.: +48 34 3250610; fax: +48 34 3250795.

E-mail address: [mdospial@wp.pl](mailto:mdospial@wp.pl) (M. Dospial).

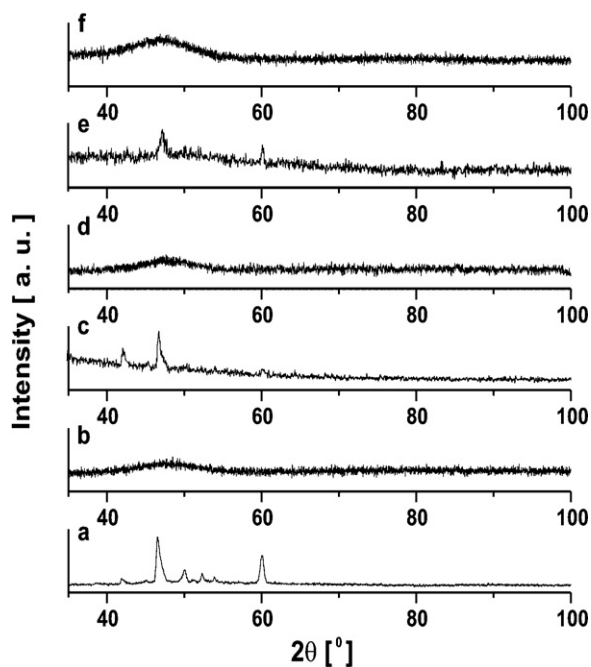


**Fig. 1.** X-ray diffraction patterns for the bulk amorphous  $\text{Fe}_{61}\text{Co}_{10}\text{Zr}_{2+x}\text{Hf}_{3-x}\text{W}_2\text{Y}_2\text{B}_{20}$  ( $x=1$  (a, d), 2 (b, e) or 3 (c, f)) alloy in the as-quenched state, in the form of plates (a–c), and rods (d–f).

The samples were obtained in the form of rods with diameter of 1 mm and length of about 20 mm, and plates with thickness of 0.5 mm and surface area of about  $10\text{ mm} \times 10\text{ mm}$ . The entire production process was carried out under a protective argon atmosphere.

The microstructure of the as-quenched samples was verified using a “Bruker” X-ray diffractometer, a “POLON” Mössbauer spectrometer and a scanning electron microscope SUPRA 25 ZEISS. Measurements of the static hysteresis loops were performed using a “Lake Shore” vibrating sample magnetometer (VSM) under the influence of magnetic fields of up to 2 T. Core losses of the investigated samples were determined from measurements performed using a FERROTESTER ferrometer. The Curie temperatures were derived as a temperature dependent function of the saturation of magnetization, using the equation  $\mu_0 M_S = \mu_0 M_0 (1 - T/T_C)^\beta$ , where  $\beta = 0.36$  is the critical exponent,  $M_0$  is the saturation of magnetization for  $T = 0\text{ K}$ , and  $\mu_0$  is the permeability of free space. The mechanical properties of all investigated samples were measured using a FutureTech 710 micro-hardness system with 0.2 kgf load (in the form of a pyramid) and over a 6 s time-period. Comparing marks left by the load on the samples (both amorphous and crystalline), allowed the determination of the wear resistance of the investigated alloys. The densities of the samples were derived using Archimedes’ Law by a fluid displacement method. The samples were weighed in air and toluene. Toluene was used, because of its well specified density variation with temperature.

### 3. Results and discussion

X-ray diffraction patterns were obtained for the investigated samples of the  $\text{Fe}_{61}\text{Co}_{10}\text{Zr}_{2+x}\text{Hf}_{3-x}\text{W}_2\text{Y}_2\text{B}_{20}$  (where  $x=1, 2$  or 3) alloy in the forms of plates and rods in the as-quenched state, as shown in Fig. 1.

On the sets of X-ray diffraction patterns corresponding to the investigated  $\text{Fe}_{61}\text{Co}_{10}\text{Zr}_{2+x}\text{Hf}_{3-x}\text{W}_2\text{Y}_2\text{B}_{20}$  alloys ( $x=1, 2$  or 3) in the shape of plates with a thickness of 0.5 mm (Fig. 1b, d and f) it can be seen that all samples have an amorphous structure. For the amorphous materials it is not possible to match a pattern, as in the case of crystalline materials, whose construction can now be described with a single, repeated throughout the volume of the material, crystal. Therefore, on the X-ray diffraction patterns (Fig. 1b, d and f) measured for samples in the form of plates, are visible only broad diffuse maxima, confirming the absence of grains of crystalline phase in a volume of these samples. On diffraction patterns obtained for samples in the form of rods (Fig. 1a, c and e) narrow peaks can be clearly seen, demonstrating the presence

**Table 1**

Data obtained from the  $M$ – $H$  dependence measurements for the  $\text{Fe}_{61}\text{Co}_{10}\text{Zr}_{2+x}\text{Hf}_{3-x}\text{W}_2\text{Y}_2\text{B}_{20}$  alloy (where  $x=1, 2$  or 3):  $H_C$ , coercivity;  $\mu_0 M_S$ , saturation magnetization.

	$\mu_0 M$ [T]	$H_C$ [A/m]
Plate form		
$x=3$	1.02	1.5
$x=2$	1.03	2.6
$x=1$	1.09	5.1
Rod form		
$x=3$	0.98	1229
$x=2$	0.91	823
$x=1$	0.65	366

of crystalline phase. On the basis of Fig. 1a, c and e it can be concluded that the ability of the glass transition in such types of alloys decreases with increasing Hf substitution for Zr.

The Mössbauer spectroscopy performed using  $^{57}\text{Co}$  radiation source give information about phase composition for crystalline phases with iron content [12]. Applying this method for Fe-based amorphous alloys will allow to obtain a transmission Mössbauer spectra from which can be concluded the absence of long-range ordering between atoms [13].

Fig. 2 presents three Mössbauer spectra (Fig. 2a–c) and corresponding to them hyperfine magnetic field distributions on Fe sites (Fig. 2d–f). For all the measured samples, spectra were almost similar, consisted of one Zeeman sextet composed of wide, asymmetric, overlapping lines typical for amorphous ferromagnets. In the case of the presented spectra it was not possible to fit additional sextet corresponding to the crystalline phase characterized by narrow distribution proving the presence of a crystalline phase in amorphous matrix.

The analyses of presented transmission Mössbauer spectra were performed using a commercially available program named “NORMOS” [14]. From this analysis the corresponding to these spectra hyperfine field distributions were derived. All distributions of hyperfine fields are fairly symmetrical, but it can be distinguish at least two components, high and low field component, corresponding to the areas rich and poor in Fe, which confirms the metastable nature of these alloys.

The results clearly indicate that in the investigated bulk amorphous materials in the as-cast state, there are fluctuations in the distribution of densities of atoms. The existence in the volume of the examined alloys areas with a variable-densities can be treated as a confirmation of the results presented in [15], which refers to groups of atoms forming the large clusters, which after delivering even a small portion of energy are rebuilding in embryos or grains of the crystalline phase. The presence of such areas with a variable number of Fe neighbors may significantly affect the magnetic properties of these alloys, namely the magnetic interaction between Fe and Co atoms. As we know, the first emerging crystalline phases in these types of alloys are  $\alpha$ -Fe and  $\alpha$ -FeCo, i.e. one that can be identified using Mössbauer spectroscopy, which is much more sensitive in comparison with the X-ray diffraction. The emergence of discrete values of hyperfine field  $B_{\text{hf}} > 32\text{ T}$  would be a proof of the existence of  $\alpha$ -Fe or  $\alpha$ -FeCo phases. As it can be seen on distributions of hyperfine fields induction at  $^{57}\text{Fe}$  sites (Fig. 2d–f) there was no presence of such components. Data obtained from the analysis of Mössbauer spectra are presented in Table 2.

Fracture structure examination using the de-cohesion method, by means of scanning electron microscopy, are shown in Fig. 3.

For all the images of the structure, corresponding to the selected areas of the studied alloys in the form of plates, predominates cross-section of a smooth type (Fig. 3a–c). In Fig. 3a the mixed-type of cross-section can be seen. It consists of a smooth surface and evenly spaced fairly well developed flakes, locally spitted

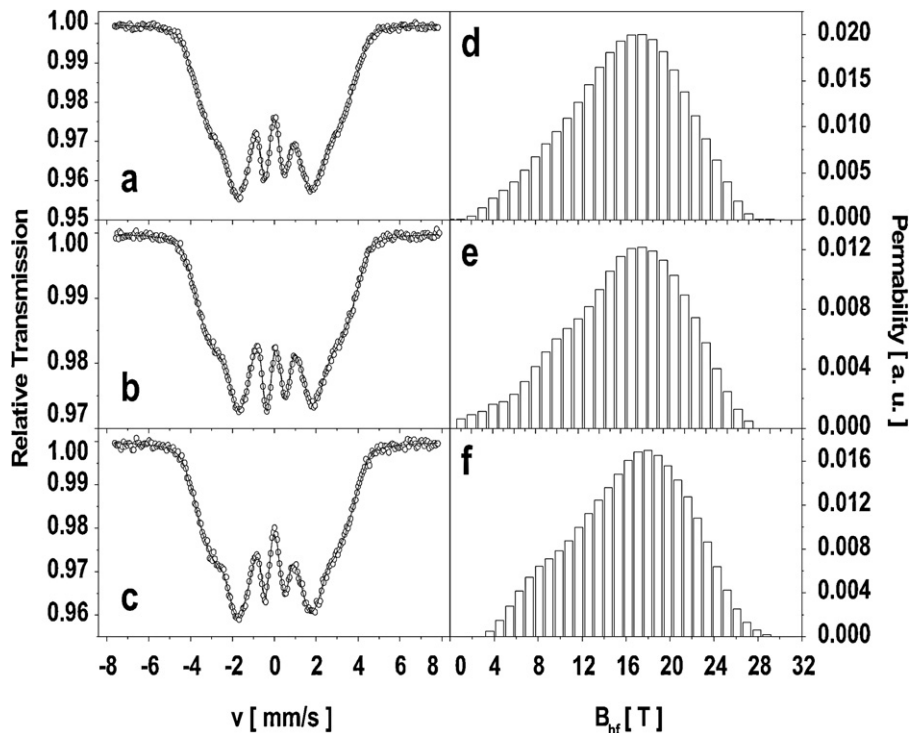


**Fig. 2.** Transmission Mössbauer spectra (a–c) and corresponding hyperfine field distribution (d–f) for  $\text{Fe}_{61}\text{Co}_{10}\text{Zr}_{2+x}\text{Hf}_{3-x}\text{W}_2\text{Y}_2\text{B}_{20}$  (where  $x=1$  (a, d), 2 (b, e) or 3 (c, f)) alloy in the form of plates.

into single veins. On the cross-section presented in Fig. 2b it can be seen the densely occurring sparsely branched, thin veins. The smoothest cross-section of the sample was observed for the alloy with  $\text{Fe}_{61}\text{Co}_{10}\text{Zr}_5\text{W}_2\text{Y}_2\text{B}_{20}$  composition. On all presented in Fig. 2 structures, next to the smooth uniform surface can be observed small areas corresponding to the presence of small bubbles. Examining the cross-section using SEM did not revealed that alloy contain grains of crystalline phase.

The static hysteresis loops measured for samples of  $\text{Fe}_{61}\text{Co}_{10}\text{Zr}_{2+x}\text{Hf}_{3-x}\text{W}_2\text{Y}_2\text{B}_{20}$  (where  $x=1, 2$  or 3) in the as-quenched state are shown in Fig. 4.

From the hysteresis loops (Fig. 4) the magnetic properties were designated and presented in Table 1.

The saturation of the magnetization for all the materials in an amorphous state are practically the same and are equal approximately 1.05 T. This allows us to conclude that Hf substitution for Zr does not affect the saturation of the magnetization. The obtained results are not comparable with those obtained by Makino et al. [16] who, for the alloys with similar compositions, have received saturation of the magnetization of about 1.5 T.

As for the coercivity field  $\mu_0 H_c$  the results indicate that 1–3% Hf substitution for Zr in alloy atomic composition, decreases the coercivity field. The Mössbauer studies have shown for the investigated materials in the form of plates lack of uniformity in the distribution of iron and cobalt atoms, which have contributed to a reduction in interactions between these atoms and, ultimately could lead to a reduction of saturation of the magnetization and increased coercivity field.

**Table 2**

The wear area obtained during 1 h wear resistance tests for the investigated samples in the form of crystalline ingots and amorphous plates.

State	$x=3$ [mm <sup>2</sup> ]	$x=2$ [mm <sup>2</sup> ]	$x=1$ [mm <sup>2</sup> ]
Crystalline	909.5	688.7	462.0
Amorphous	1081.6	806.0	552.2

The coercivity field measured for partially crystallized rods (Fig. 4b) have values in the range from 366 A/m to 1229 A/m. The reason for increase in coercivity fields is caused by the presence of magnetocrystalline anisotropy resulting from formation of the grains of crystalline phase as a result of prolonged solidification time of a liquid alloy [17]. From the data presented in Table 1 it can be concluded, that the formation of the grains of crystalline phase or phases is the fastest for the alloy with 5% of Zr content.

The Curie temperature is a very important parameter indicating stability of the ferromagnetic state of materials. In Fig. 5 the dependencies  $\mu_0 M(T)$  and  $[\mu_0 M(T)]^{1/\beta}$  are presented. From these measurements, Curie temperatures were derived for the investigated samples in the form of plates of  $\text{Fe}_{61}\text{Co}_{10}\text{Zr}_{2+x}\text{Hf}_{3-x}\text{W}_2\text{Y}_2\text{B}_{20}$  (where  $x=1, 2$  or 3) alloy.

The calculated Curie temperatures for the investigated samples in the form of plates were about: 520 K, 526 K and 506 K, for  $x=3, 2$  and 1, respectively. The determination of a discrete value of Curie temperature ( $T_C$ ) for amorphous materials is hindered because of the existence of regions with different iron concentration within the volume of the sample. The existence of these regions was confirmed by Mössbauer spectroscopy measurements. The lack of the clearly specified value of the Curie temperature means that transformation from the ferro- to paramagnetic state is gradual, and depends to a great extent on the degree of relaxation of the material's structure.

The other important parameters which determine the applications for soft magnetic materials are: permeability and core losses. From measurements carried out using a fully automatic ferrometer, the maximal magnetic permeability (at constant frequency  $f=500$  Hz) and core losses (at constant maximal magnetic induction  $B_{\text{max}}=0.2$  T) were derived for all investigated samples in the form of plates (Fig. 6).

The highest value of the maximal magnetic permeability ( $\mu=1825$ ) was achieved in a magnetic field of  $H=46$  A/m for  $\text{Fe}_{61}\text{Co}_{10}\text{Zr}_5\text{W}_2\text{Y}_2\text{B}_{20}$  alloy. For the two remaining alloys,  $\text{Fe}_{61}\text{Co}_{10}\text{Zr}_4\text{Hf}_1\text{W}_2\text{Y}_2\text{B}_{20}$  and  $\text{Fe}_{61}\text{Co}_{10}\text{Zr}_3\text{Hf}_2\text{W}_2\text{Y}_2\text{B}_{20}$ , values of

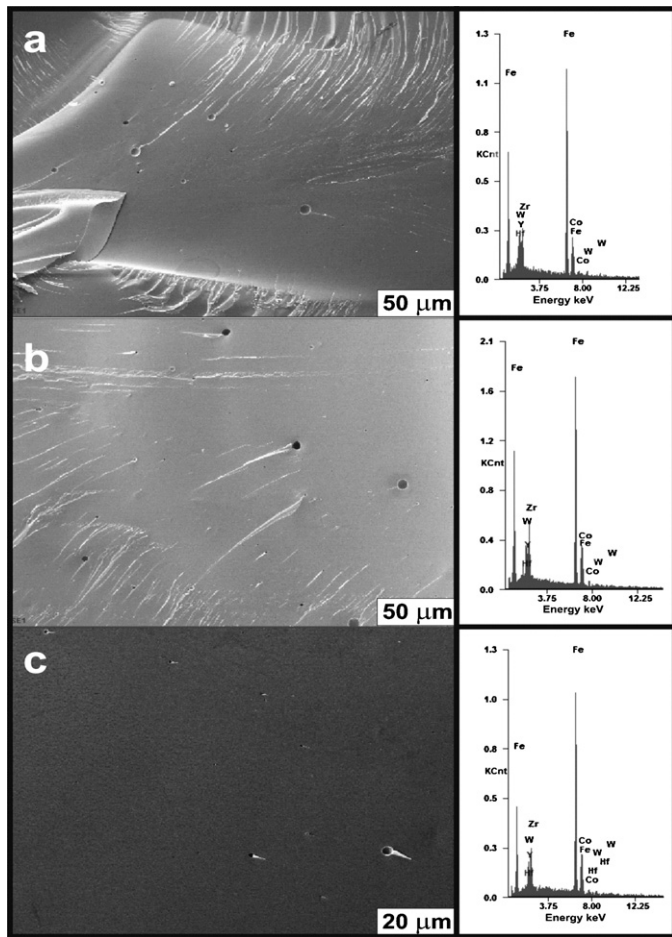


Fig. 3. The selected areas of the cross-section obtained by decohesion with the corresponding spectrograms for  $\text{Fe}_{61}\text{Co}_{10}\text{Zr}_{2+x}\text{Hf}_{3-x}\text{W}_2\text{Y}_2\text{B}_{20}$  (where  $x = 1$  (a), 2 (b) and 3 (c)) alloys in the form of plates with a thickness of 0.5 mm.

the maximal magnetic permeability were 1708 (at  $H = 39 \text{ A/m}$ ) and 1572 (at  $H = 35 \text{ A/m}$ ). It may be concluded as hafnium content increases (hence zirconium content decreases) there is a concomitant decrease in the maximal magnetic permeability value and a shift of the peak value towards lower magnetic fields. Similarly, the values of core losses decrease with increasing hafnium content (Fig. 6b).

On the basis of the performed magnetic measurements, it can be stated that obtained bulk amorphous alloys have very good soft magnetic properties. In addition, the investigated amorphous materials are characterized by significantly higher values of microhardness in comparison with their crystalline counterparts. The microhardness was measured for crystalline ingots, partially crystallized rods and amorphous samples in plate-form. Fig. 7 depicts examples of the imprints obtained using the Vickers method.

The bulk amorphous materials, presented in this work, are showing fairly good soft magnetic properties and have significantly higher microhardness compared with their crystalline counterparts of the same chemical compositions. The study of microhardness was carried out for crystalline ingots, partially crystallized rods and amorphous plates.

Microhardness of the crystalline ingots, for all the investigated alloys is much smaller than for the samples obtained by radial cooling of a liquid alloy, in the water-cooled copper mould. Such an improvement of mechanical properties for partially crystallized and amorphous samples is associated with a higher packing-density of the atoms in the amorphous matrix.

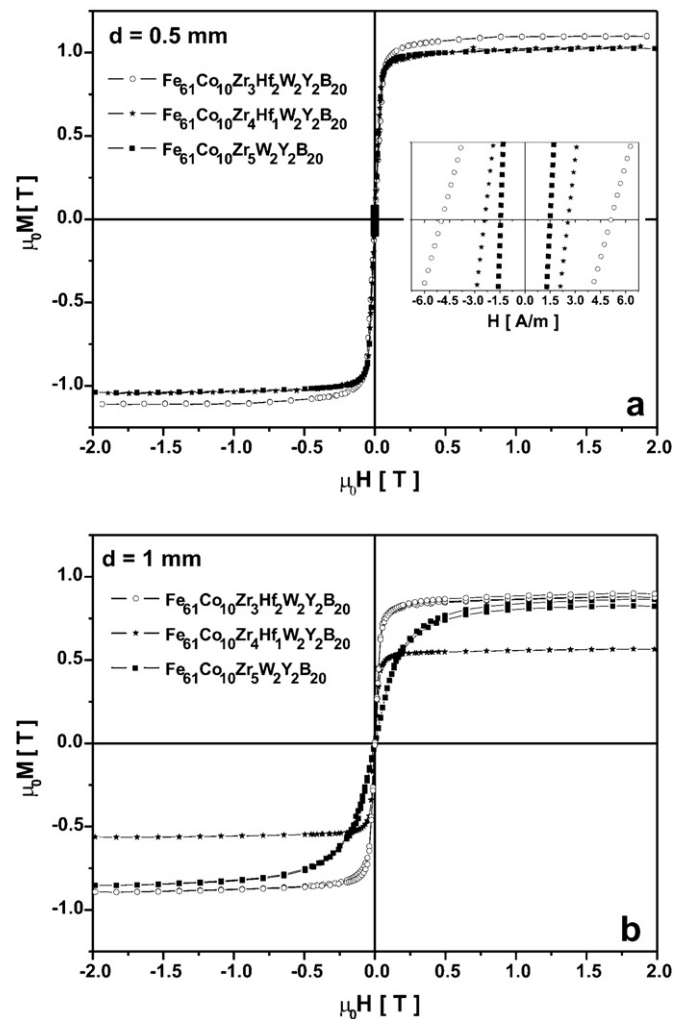


Fig. 4. Static hysteresis loops for  $\text{Fe}_{61}\text{Co}_{10}\text{Zr}_{2+x}\text{Hf}_{3-x}\text{W}_2\text{Y}_2\text{B}_{20}$  alloy in the as-quenched state: in the form of plates (a) and rods (b).

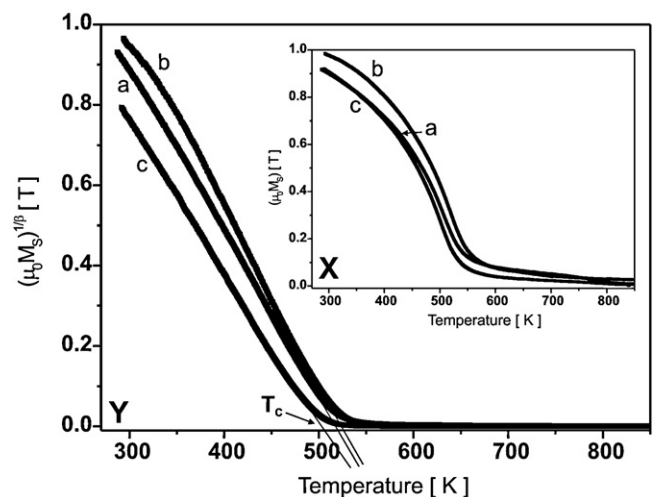
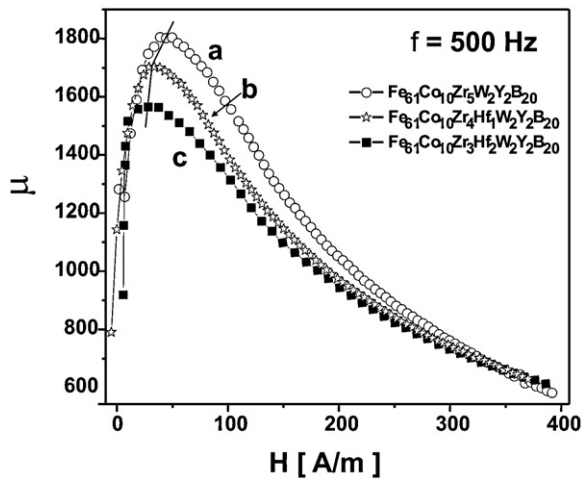


Fig. 5. The temperature dependence of the saturation of magnetization and  $(\mu_0 M_S)^{1/\beta}$  curves, measured for  $\text{Fe}_{61}\text{Co}_{10}\text{Zr}_{2+x}\text{Hf}_{3-x}\text{W}_2\text{Y}_2\text{B}_{20}$  alloy in plate-form:  $x = 1$  (c),  $x = 2$  (b) and  $x = 3$  (a).



**Fig. 6.** The magnetic field dependence of maximal magnetic permeability (a) and frequency dependence of core losses (b) for  $\text{Fe}_{61}\text{Co}_{10}\text{Zr}_{2+x}\text{Hf}_{3-x}\text{W}_2\text{Y}_2\text{B}_{20}$  alloys in the as-quenched state in the form of plates:  $x = 1$  (c), 2 (b) or 3 (a).

The highest microhardness was obtained for the samples in the form of plates, slightly lower its values were obtained for the partly crystallized rods. The value of the microhardness is described by resistance of the material, to force applied using the polygon prism with an angle of  $136^\circ$ , acting perpendicular to the surface. This value is directly dependent on the energy state of the surface and is proportional to stress in subsurface zone. The stress in a bulk amorphous materials, is the result of rapid solidification, the cooling speed is much greater than for materials with a crystalline structure. In the rapid solidification process a large temperature gradient, between the temperature of the core and the sample surface is present. That results in higher tensile stresses in the subsurface zone. Therefore, for the investigated materials with an amorphous structure, the higher values of microhardness,

**Table 3**

The microhardness values of the investigated samples in the form of: crystalline ingots ( $Hv_{\text{cryst}}$ ), amorphous plates ( $Hv_{\text{am(pl)}}$ ) and amorphous rods ( $Hv_{\text{am(rd)}}$ ). Also, the theoretical ( $\rho_{\text{th}}$ ) and experimental ( $\rho_{\text{ex}}$ ) density values and the relationship between them ( $\rho_{\text{th}}/\rho_{\text{ex}}$ ) for the amorphous samples in the form of plates.

Alloy	$Hv_{\text{cr}}$	$Hv_{\text{am(pl)}}$	$Hv_{\text{am(rd)}}$	$\rho_{\text{th}}$ [ $\text{g}/\text{cm}^3$ ]	$\rho_{\text{ex}}$ [ $\text{g}/\text{cm}^3$ ]	$\rho_{\text{th}}/\rho_{\text{ex}}$
$x = 3$	783	1122	1174	6.96	7.61	1.09
$x = 2$	788	1159	1174	7.08	8.05	1.13
$x = 1$	779	1129	1140	7.10	8.30	1.16

than for alloys with the same chemical compositions but with the crystalline structure, were obtained.

The amorphous materials usually possess a greater value of wear resistance than their crystalline counterparts. Examples of wear areas, created during the wear resistance test, are shown in Fig. 8.

The summarized mechanical properties, gained during the wear resistance test, are listed below in Table 2.

From analysis of the data, it can be seen that crystallized ingots of all the investigated materials have greater values of wear resistance than their amorphous equivalents in the plate-form. The tests were repeated several times, and the results were similar. For all the investigated alloys, the mechanical properties were closely related with their chemical composition. Both wear resistance and microhardness values were found to change as hafnium atoms were replaced by zirconium atoms. Even a small change in Hf content ( $13.29 \text{ g}/\text{cm}^3$ ) to Zr ( $6.51 \text{ g}/\text{cm}^3$ ) resulted in an increase in wear resistance and, unfortunately, a slight decrease in microhardness.

Using Archimedes' Law, the densities were calculated for the investigated materials which were in the forms of crystalline ingots and amorphous plates. The evaluated densities of the investigated alloys were found to increase with increasing Hf content. In Table 3, the results of the microhardness tests and density values for the investigated samples are summarized.

The relationship  $\rho_{\text{th}}/\rho_{\text{ex}}$  determines the packing-density of the atoms in the alloy. Other researchers have shown that metallic

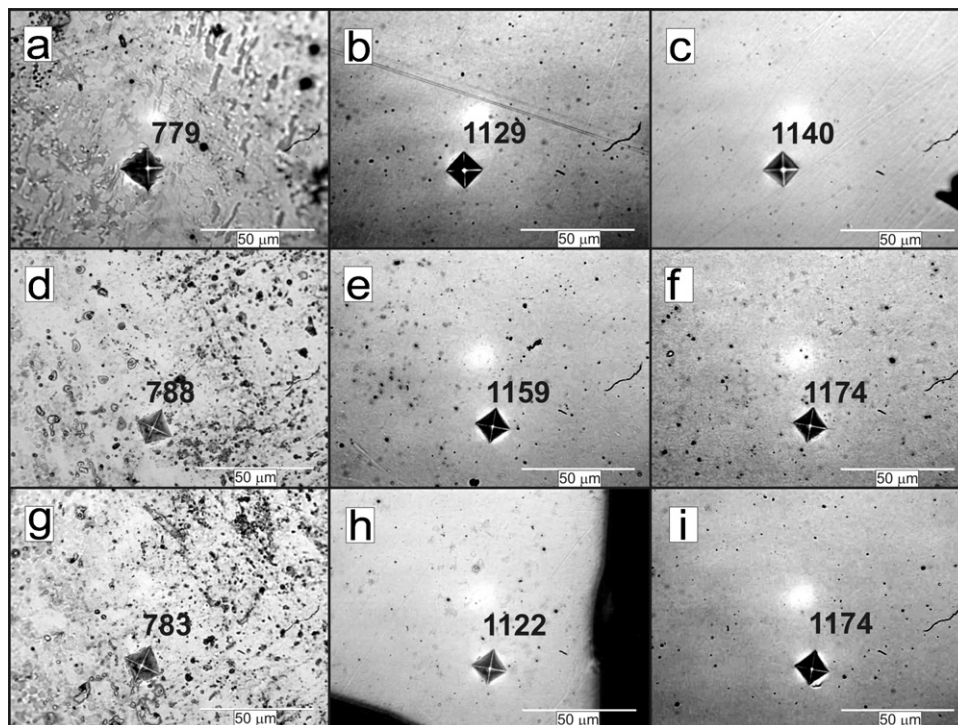


**Fig. 7.** Imprints of load from the microhardness test for  $\text{Fe}_{61}\text{Co}_{10}\text{Zr}_5\text{W}_2\text{Y}_2\text{B}_{20}$  where  $x = 1, 2$  or  $3$  alloy in the form of crystalline ingots (a, d and g), partially crystallized rods (b, e and h) and amorphous plates (c, f and i), respectively (a–c,  $x = 1$ ; d–f,  $x = 2$ ; g–i,  $x = 3$ ).

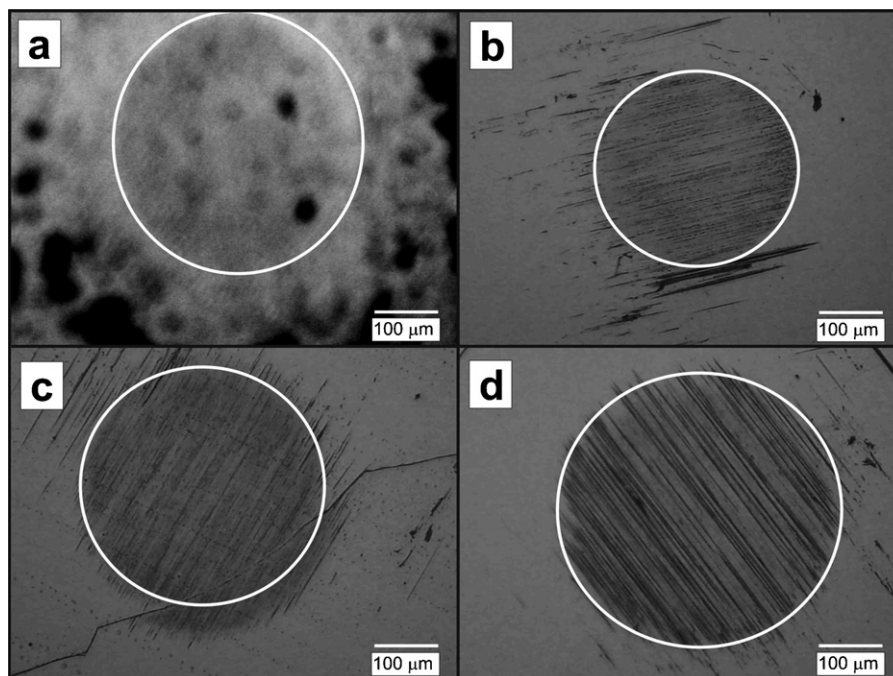


**Fig. 8.** Examples of wear areas for the investigated samples of  $\text{Fe}_{61}\text{Co}_{10}\text{Zr}_{2+x}\text{Hf}_{3-x}\text{W}_2\text{Y}_2\text{B}_{20}$  alloy in the form of amorphous plates (for  $x = 1$  (d), 2 (c) or 3 (d)) and crystalline ingot (for  $x = 1$  (a)).

glasses with a greater value of packing density have a greater glass forming ability and microhardness [18–20]. In comparison with their crystalline equivalents, the investigated alloys have lower values of wear resistance (Fig. 8).

#### 4. Conclusions

The studies of structure showed that suction-casting method allow to obtain  $\text{Fe}_{61}\text{Co}_{10}\text{Zr}_{2+x}\text{Hf}_{3-x}\text{W}_2\text{Y}_2\text{B}_{20}$  ( $x = 1, 2$  or  $3$ ) bulk amorphous samples in the form of plates with 0.5 mm thickness. The samples in the form of rods with diameter of 1 mm produced using same alloy composition and production method were partially crystallized.

The partially crystallized sample with lowest Zr content in atomic composition was characterized by best soft magnetic properties and lowest content of crystalline phase in sample volume, what allows us to suppose that this alloy has the best glass transition ability.

The Curie temperature for all investigated alloys in the form of plates are quite high, averaging about 520 K, which means that these materials can be successfully used in electrical equipment operating at elevated temperatures.

Permeability for the investigated alloys with amorphous structure decreases with increasing Hf content, the reverse as the core loses. The investigated materials were also characterized by the relatively high saturation of the magnetization, which practically does not depend on the Zr and Hf content, at least for the described in this article content of these elements. Even a small percentage change of these elements in the atomic composition of an alloy determines the strength of coercivity field. In amorphous materials magnetocrystalline anisotropy is not observed, which means that the coercivity field should be small and for the investigated materials have a value equal to only a few A/m.

It should also be pointed out that the structure of an amorphous materials, showed much higher micro-hardness, than their crystalline equivalents with the same alloy compositions. That was a result of the higher packing density of atoms per volume unit.

In summary, the best soft magnetic characteristics were obtained for the alloy with 5% Zr content. In addition, these alloys also show a relatively high microhardness.

#### References

- [1] Z.H. Gan, J.J. Fu, J. Liu, J.Z. Xiao, *J. Alloys Compd.* 459 (2008) 504–507.
- [2] K.F. Yao, C.Q. Zhang, *Appl. Phys. Lett.* 90 (2007) 61901–61911.
- [3] Y. He, R.B. Schwarz, J.I. Archuleta, *Appl. Phys. Lett.* 69 (1996) 23.
- [4] A. Inoue, *Acta Mater.* 48 (2000) 279–306.
- [5] W.H. Wang, M.X. Pan, D.Q. Zhao, Y. Hu, H.Y. Bai, *J. Phys.: Condens. Matter* 16 (2004) 3719–3723.
- [6] M. Iqbal, J.I. Akhter, H.F. Zhang, Z.Q. Hu, *J. Non-Cryst. Solids* 354 (2008) 3284–3290.
- [7] T.A. Aycan, M. Baricco, *J. Alloys Compd.* 434–435 (2007) 176–179.
- [8] H.E. Khalifa, J.L. Cheney, K.S. Vecchio, *Mater. Sci. Eng. A* 490 (2008) 221–228.
- [9] A. Hernando, M. Vázquez, in: H.H. Liebermann (Ed.), *Rapidly Solidified Alloys*, Marcel Dekker, New York, 1993, p. 560.
- [10] M.E. McHenry, M.A. Willard, D.E. Laughlin, *Prog. Mater. Sci.* 44 (1999) 291.
- [11] G.E. Fish, *IEEE Proc.* 78 (1990) 947.
- [12] J. Olszewski, *Serie Monografie nr 119*, Wydawnictwo Politechniki Czestochowskiej, Czestochowa, 2006 (in Polish).
- [13] J. Frąckowiak, Ph.D. Thesis, 1994 (in Polish).
- [14] R.A. Brand, “Normos-90”, Universität Duisburg, 2002.
- [15] M. Stoica, R. Li, A.R. Yavari, G. Vaughan, J. Eckert, N. Van Steenberghe, D.R. Romera, Thermal stability and magnetic properties of FeCoBSiNb bulk metallic glasses, *Journal of Alloys and Compounds* 504S (2010) S123–S128.
- [16] A. Makino, T. Kubota, Ch. Chang, M. Makabe, A. Inoue, *J. Magn. Magn. Mater.* 320 (2008) 2499–2503.
- [17] D.Y. Liu, W.S. Sun, H.F. Zhang, Z.Q. Hu, *Intermetallics* 12 (2004) 1149–1159.
- [18] Y. Liu, H. Bei, C.T. Liu, E.P. George, *Appl. Phys. Lett.* 90 (2007) 071909.
- [19] A. Concustell, G. Alcalá, S. Mato, T.G. Woodcock, A. Gerbert, J. Eckert, et al., *Intermetallics* 13 (2005) 1214–1219.
- [20] B. Yao, Y. Zhang, L. Si, H. Tan, Y. Li, *J. Phys.: Condens. Matter* 16 (2004) 6325–6335.